Hindawi Publishing Corporation
EURASIP Journal on Bioinformatics and Systems Biology
Volume 2007, Article ID 46150, 9 pages
doi:10.1155/2007/46150

Research Article

Computational Methods for Estimation of Cell Cycle Phase Distributions of Yeast Cells

Antti Niemistö,[1] Matti Nykter,[1] Tommi Aho,[1] Henna Jalovaara,[2] Kalle Marjanen,[1] Miika Ahdesmäki,[1] Pekka Ruusuvuori,[1] Mikko Tiainen,[2] Marja-Leena Linne,[1] and Olli Yli-Harja[1]

[1] *Institute of Signal Processing, Tampere University of Technology, P.O. Box 553, 33101 Tampere, Finland*
[2] *MediCel Ltd., Haartmaninkatu 8, 00290 Helsinki, Finland*

Received 30 June 2006; Revised 5 March 2007; Accepted 17 June 2007

Recommended by Yidong Chen

Two computational methods for estimating the cell cycle phase distribution of a budding yeast *(Saccharomyces cerevisiae)* cell population are presented. The first one is a nonparametric method that is based on the analysis of DNA content in the individual cells of the population. The DNA content is measured with a fluorescence-activated cell sorter (FACS). The second method is based on budding index analysis. An automated image analysis method is presented for the task of detecting the cells and buds. The proposed methods can be used to obtain quantitative information on the cell cycle phase distribution of a budding yeast *S. cerevisiae* population. They therefore provide a solid basis for obtaining the complementary information needed in deconvolution of gene expression data. As a case study, both methods are tested with data that were obtained in a time series experiment with *S. cerevisiae*. The details of the time series experiment as well as the image and FACS data obtained in the experiment can be found in the online additional material at http://www.cs.tut.fi/sgn/csb/yeastdistrib/.

1. INTRODUCTION

Many recent studies have concentrated on the construction of dynamic models for genetic regulatory networks [1–4]. In such studies, the gene expression levels of cell-cycle-regulated genes are observed as time series with a relatively short sampling interval over a relatively long period of time. Because currently it is difficult to profile single cells, time series microarray experiments are usually carried out by synchronizing a population of cells. In a synchronous cell population, all cells are initially in the same phase of the cell cycle. Regardless of the synchronization method, synchrony of the cell population is lost over time. For the budding yeast *Saccharomyces cerevisiae*, cells seem to remain relatively synchronized for two cell cycles [5], although the loss of synchrony is a continuous process, and the cells are much less synchronized in the second cell cycle than in the first cycle.

The unavoidable asynchrony of the cell population results in that the measured gene expression level is in fact an average of the true values of the neighboring cell cycle phases. In the case of a relatively synchronous population, this effect can be modeled by convolution. Moreover, if the cell cycle phase distribution of the cell population can be estimated, the blurring effect of convolution can be inverted to obtain an estimate of the true expression level that would have been obtained in a hypothetical perfectly synchronized experiment. In the case of the budding yeast, several different approaches have been proposed for this task [6, 7]. These studies have concentrated on the deconvolution task. However, since the quality of the obtained estimate of the true expression levels depends on the quality of the estimate of the cell cycle phase distribution, we concentrate here on the distribution estimation.

There are two basic approaches to estimating the cell cycle phase distribution of a cell population. In the first one, the numbers of cells that are in different phases of the cell cycle are found for one time instant or a short time interval. The result is an age distribution of the cell population. In the second approach, the number of cells that are in a given phase of the cell cycle is monitored over time. The result is a time distribution of the cell population. Both types of distribution estimates can be used for the deconvolution task [6, 7].

A fluorescence-activated cell sorter (FACS) is a device that can be used to measure the DNA content of a single cell with the aid of fluorescence dyeing. It produces a histogram of DNA content in the cells under investigation. In earlier studies with budding yeast [5, 7, 8], an estimate for the cell cycle phase distribution of a cell population has been

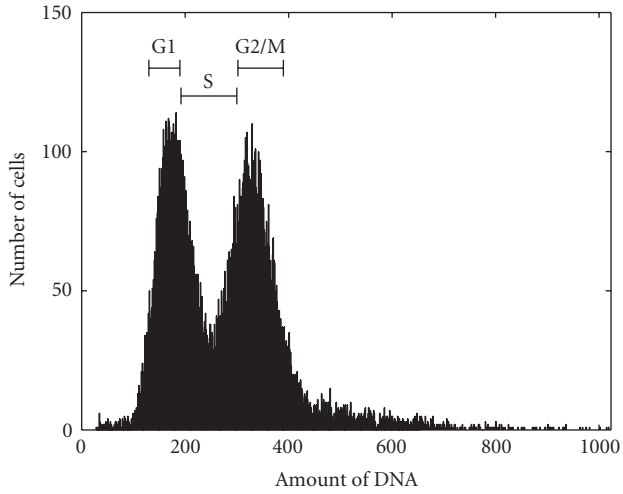

Figure 1: The conventional method for determining the number of cells in each phase of the cell cycle by using a FACS histogram. This is an example of an asynchronous cell population; there are 27, 27, and 26 percent of cells in cell cycle phases G1, S, and G2/M, respectively.

obtained from the FACS histogram by counting the number of cells in different phases. This has been done manually by marking the range of each phase in the FACS histogram and counting the number of cells in that range, see Figure 1. The results obtained with this approach are dependent on the method used to determine the location of each phase. It is also difficult to obtain a good estimate for the S phase of the cell cycle with this approach [9].

The phase of the cell cycle depends by definition on the amount of DNA in the cell. Cells that are in the G1 phase have the DNA amount N, whereas cells in the G2/M phase have the amount $2N$. In the S phase, the amount of DNA is between N and $2N$. In this study, we further assume that the size of a bud of a dividing cell depends on the phase of the cell cycle [5, 7, 10]. Cells that are in the G1 phase are assumed not to have a bud, cells that are in the S phase are assumed to have a small bud, and cells that are in the G2/M phase are assumed to have a large bud. Based on these assumptions, we propose two computational high-throughput methods for estimating the cell cycle phase distribution of a budding yeast cell population. Some preliminary results have been published in conference proceedings [11, 12].

The first estimation method is a nonparametric method, in which the estimate of the age distribution is obtained by analyzing the amount of DNA in the cells with a FACS. The method has two stages. At the first stage, we use FACS data from an asynchronous cell population for estimating the rate of DNA replication in a cell. This estimate can then be used to find the age distribution of a cell population whose FACS histogram is known. The population whose distribution is estimated can be synchronized or it can be otherwise aligned so that its age distribution is different from a wild-type population. In the second method, the estimate of the time distribution is obtained by performing budding index analysis through image analysis. The method is developed for images taken with a light microscope without any fluorescence staining, which makes the image analysis significantly more difficult than if fluorescent micrographs were used [13]. Also, in contrast to earlier studies where the image analysis is performed manually through visual inspection of the cells [5, 7], our image analysis method is fully automated.

2. METHODS

In this section, we present two computational methods for estimation of the cell cycle phase distribution of a yeast cell population. The FACS-based method is presented in Section 2.1, and the image analysis methods needed for budding index analysis are presented in Section 2.2. It should be noted that neither of the presented methods depends on the synchronization method. In fact, the methods do not require the cell population to be synchronized at all. Thus, both methods can be directly applied to data from any experiment in which the cell cycle phase distribution of the population differs from that of a wild-type population.

2.1. Distribution estimation using FACS histograms

In a growing cell culture, the number of cells increases. As a result of cell division, two newborn cells are obtained. Thus, there are twice as many newborn as dividing cells in the culture. The age distribution of the wild-type asynchronous cell population can be modeled as $p(t) = 2^{(1-t)}$ [14]. Here, t is a discrete variable and denotes the cell cycle phase, that is, the age of the cell from the cell division, normalized to the interval $[0, 1]$ and uniformly sampled with Δt intervals as $t \in \{0, \Delta t, 2\Delta t, \ldots, 1\}$. Thus, cells divide at age 1 and newborn cells are of age 0. This distribution is shown in Figure 2(a).

Since we know the total number, N, of cells used in the FACS measurement as well as the underlying age distribution $p(t)$, we can compute the number of cells at each small time interval $[t_k - \Delta t, t_k]$, $t_k \in \{\Delta t, 2\Delta t, \ldots, 1\}$ as $c(t_k) = N(2^{(1-(t_k-\Delta t))} - 2^{(1-t_k)})$. Furthermore, the cumulative number of cells at time t is $C(t) = \sum_{i=0}^{t} c(i) = N(2 - 2^{(1-t)})$. That is, for a given t, $C(t)$ is the total number of cells at the earlier phases of the cell cycle.

As we know the cumulative number of cells $C(t)$ and have measured the histogram h_a of the DNA content of the cells (see Figure 2(b) for a simulated histogram and Figure 1 for a histogram from a real FACS measurement), we can estimate the DNA replication function, denoted by $f(t)$. This is a mapping from "*number of cells*"-"*cell cycle phase*"-space to "*number of cells*"-"*amount of DNA*"-space, see Figure 2. It can be estimated from the FACS histogram of an asynchronous population h_a by finding, for each $t \in \{0, \Delta t, 2\Delta t, \ldots, 1\}$,

$$f(t) = \arg\min_{K} \left(\left| \sum_{i=0}^{K} h_a(i) - C(t) \right| \right), \tag{1}$$

where $h_a(i)$ is the value of the FACS histogram of the asynchronous population at the point i, and $K \in \mathbb{N}$.

An example of a simulated $f(t)$ is shown in Figure 2(c). As the FACS histogram h_a is a discrete measurement of the

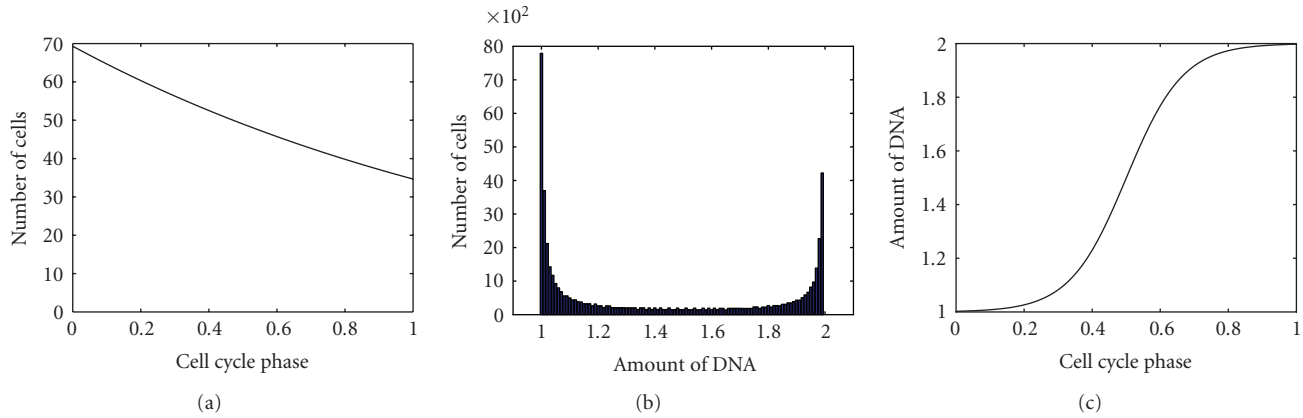

FIGURE 2: A simulated (a) distribution of an asynchronous cell population, (b) noise-free FACS histogram, and (c) DNA replication function. The details of the data simulation can be found in the online additional material [15].

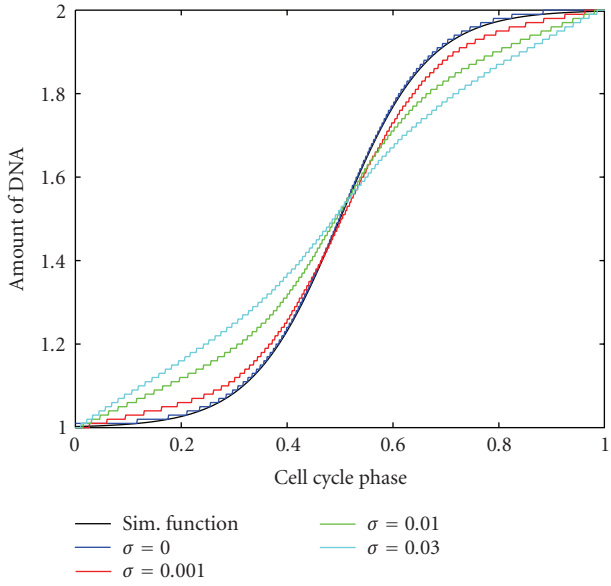

FIGURE 3: DNA replication functions estimated from simulated data with different amounts of noise. Gaussian noise with variance σ is added to the simulated data as explained in the online additional material [15].

amount of DNA, the estimated $f(t)$ is a discrete version of the true continuous DNA replication function.

Examples of the DNA replication functions estimated from simulated data under different amounts of noise are shown in Figure 3. The effect of the noise is studied by using a simple additive Gaussian noise model:

$$\hat{x} = x + e, \tag{2}$$

where $e \sim N(0, \sigma)$ and x is a noise-free DNA amount of a cell. This noise model, although simple, produces FACS histograms that resemble those measured from real data. The details of the data simulation process can be found in the online additional material [15]. Figure 3 shows that in the noise-free case the obtained discrete estimate is consistent with the underlying DNA replication function $f(t)$. As the amount of noise increases, the accuracy of the obtained estimate for DNA replication degrades. It would be possible to improve the quality of the estimate under noisy conditions by using a model-based estimation approach. However, this approach would require us to make assumptions about the form of the true DNA replication function and about the noise characteristics of FACS measurements. As neither of these are known in detail, we rely on our proposed nonparametric approach that does not make any assumptions about the characteristics of the noise or the DNA replication function.

Having obtained an estimate for the DNA replication function $f(t)$, we can estimate the age distribution of a synchronous population. We assume that the function $f(t)$ is the same for all cells, that is, for cells of synchronous as well as of asynchronous populations. This assumption is justified, because $f(t)$ represents the DNA replication of a single cell, and the behavior of a single cell is not thought to be affected by whether the population is synchronous or asynchronous.

The function $f(t)$ presents the amount of DNA that is present at each time instant of the cell cycle. Having this information, we can use the FACS histogram of a synchronous population to evaluate the number of cells that this amount of DNA corresponds to. Thus, the age distribution of the cell population is obtained by

$$x(t) = \sum_{i=0}^{f(t)} h_s(i) - \sum_{i=0}^{t-\Delta t} x(i), \tag{3}$$

where $f(t)$ is the value of the DNA replication function and $h_s(i)$ is the value from the FACS histogram of the synchronous population at the point i. The obtained age distribution is discrete, and the cell cycle phase parameter t is a discrete variable, $t \in \{0, \Delta t, 2\Delta t, \ldots, 1\}$.

When a FACS histogram from a real measurement (see Figure 1) is compared with the ideal simulated histogram (see Figure 2(b)), a significant difference is observed. As discussed in Section 1, all cells should have an amount of DNA between N and $2N$. Thus, if the histogram indicates cells

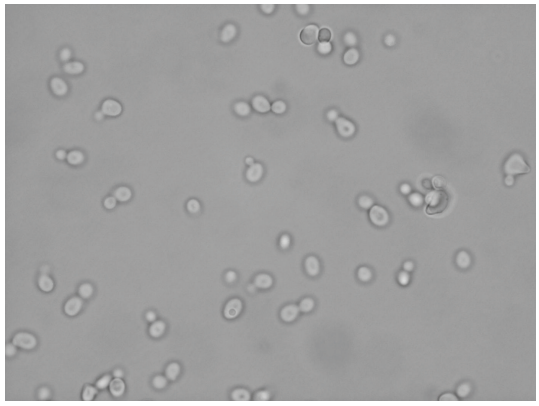

Figure 4: The green component of a microscopic image of a wild-type budding yeast cell population. The size of the image is 1388 × 1037 pixels.

having DNA amounts less than N or greater than $2N$, the respective bins can be assumed to be due to measurement errors and should be excluded from the analysis. As illustrated in Figure 1, the peaks of the histogram correspond to the G1 (DNA amount N) and G2/M (DNA amount $2N$) phases, while the area between the peaks corresponds to the S phase. Therefore, all data that are not included in these three areas should be considered as measurement errors and should be removed. The removal can be done by estimating the locations of the two highest peaks and excluding all data that are not in the range between these two peaks. This preprocessing step will make the real FACS histogram resemble the ideal simulated histogram shown in Figure 2(b).

Although the above estimation method was introduced in the context of a synchronous cell population, it can be applied to any population of yeast cells. The only requirement for the applicability of the method is that FACS measurements are available for a wild-type yeast population as well as for the population whose age distribution is being estimated. The estimated population can be a synchronized population or it can be otherwise aligned because of a perturbation.

2.2. Distribution estimation using budding index analysis

An automated image analysis method for budding index analysis is needed, because obtaining the budding index data manually through visual analysis has a number of drawbacks. One of the drawbacks is that accurate visual analysis is tedious and slow, and in a typical experiment, the number of budding yeast images for which budding index data are needed is large. Moreover, manual counting is always subjective. If visual analysis is performed a second time by the same or a different person, the results will usually not be the same as they were the first time. With automated image analysis, objectivity of the results is guaranteed because the same criteria are always used to determine if a feature in the image represents a cell or bud, and the results are therefore easily reproducible.

In budding yeast images, the cell membranes are typically clearly visible as circular or elliptic regions that are darker than the background. The image shown in Figure 4 is taken of a wild-type budding yeast population, and is used here in the presentation of the image analysis methods. Since yeast cells grow loose in a solution, the scene that is imaged in any experiment is three-dimensional. Therefore, all the cells are not visible in the two-dimensional images, because not all of them are in the same focal plane. Moreover, a bud may be hidden behind the parent cell. However, to estimate the distribution of the population, we do not need to know the real percentage of buds versus parent cells. Rather, it is enough to find the relative numbers of buds between different images. Therefore, the goal is to detect cells that are focused relatively well and to completely ignore cells that are in poor focus.

The first task is segmentation of the images in order to separate the cell membranes from the background. First, the effect of uneven illumination is removed from the image with a polynomial fit. After this, the estimates of the local mean and the local variance are computed. The resulting local mean and variance images are used to form a two-dimensional histogram. The core of the segmentation method is the subsequent clustering of the mean-variance space. The clustering is based on two assumptions. The first assumption is that the cell membranes are darker than their neighborhoods on the average. The second assumption is that if a cell is in focus, it has sharp edges, and the variance of the cell neighborhood is higher than the variance of the background of the image.

The result of clustering is a binary image in which the cell membranes are represented by ones (shown as white pixels) and the background is represented by zeros (shown as black pixels). Then, the remaining holes in the cell membranes are filled by applying the morphological closing operation with a circular structuring element inside an 11×11 square. Next, all small objects are removed. The assumption is that objects that are very small are not cells but result from artifacts in the original image. The removal is done by labeling the connected components after which it is straightforward to determine the sizes of each object and to remove them if necessary. Finally, the Euclidean distance transform is performed on the binary image to detect the inner and outer boundaries of the cell membranes. The result for the image in Figure 4 is shown in Figure 5.

It can be seen in Figure 5 that the inner boundary of the cell membrane can be used for detection of small buds. Specifically, in most cases a small bud remains connected to the parent cell, and there is bridge-like connection between the parent cell and the bud. A good example is shown in Figure 6, which shows a part of the image in Figure 4 at different image processing stages (see below). On the other hand, the inner boundaries of larger buds are usually disconnected from the inner boundaries of the parent cell. Buds that are separated from the parent cell in the segmentation result can thus be detected based on the sizes and numbers of objects (inner boundaries of a cell membrane) that are inside the outer boundary of a cell membrane.

Before any cells or buds are detected, all objects (cell membranes) that touch the edges of the image are removed

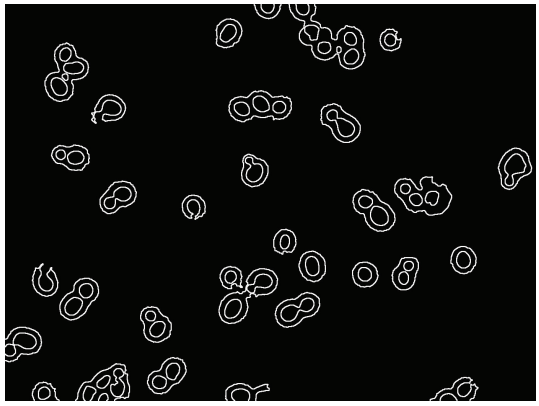

Figure 5: The segmentation result of the image in Figure 4. The inner and outer boundaries of the cell membranes of the cells are shown on a black background.

from the image, because it is not realistic to estimate the sizes of objects that are not completely seen in the image. The next step is to remove all outer boundaries of the cell membranes. Since there are now no objects touching the edges of the image, a simple flood-fill can be performed from any pixel at the edge of the image, after which the outer boundaries can be removed by removing the object that touches the edges of the image. Some objects that are not in good focus in the original image only have a horseshoe-like outer boundary with no inner boundary, and thus they get removed here, too. One example of this can be seen near the upper left corner of the image in Figure 4.

Next, the objects are filled to obtain the image in Figure 7. This is based on labeling the connected components of the complement image (black and white reversed). In the labeled complement image, the component that touches the edges of the image corresponds to the background, and all the other components correspond to cell regions that need to be filled in the original image. The filling is then done according to the labels of the connected components.

Separation of buds from the parent cells is done with a modification of the object separation method that has been proposed in [16]. The method is based on two criteria of the objects. The first one is a compactness measure:

$$c = \frac{4\pi A}{p^2}, \tag{4}$$

where A is the area of an object and p is the length of its boundary line, that is, its perimeter. Both of these can be measured in pixels, but note that c is a dimensionless quantity. The compactness can be computed efficiently using the chain code representation of objects. Objects that have a low compactness are candidates for objects that represent cells that have a small bud. The second criterion is calculated in the case of bud separation only for objects for which $c < 0.6$. It is given by

$$r = \max_{\mathbf{x}_1,\mathbf{x}_2 \in B} \frac{l_b(\mathbf{x}_1, \mathbf{x}_2)}{l_d(\mathbf{x}_1, \mathbf{x}_2)}, \tag{5}$$

where $\mathbf{x}_1 = (x_1, y_1)$ and $\mathbf{x}_2 = (x_2, y_2)$ are the coordinates of two points on the boundary of the object, B is the set of boundary coordinates, l_b is the distance between the points along the boundary of the object, and l_d is the Euclidean distance between the points. In the case of bud separation, a cutline is drawn between the corresponding boundary coordinates if $r > 3.5$. The threshold values of c and r were obtained in iterative tests with different threshold values and different images.

The result of applying the object separation method to the image of Figure 7 is shown in Figure 8, in which the buds are marked with the red color. It can be seen that all small buds are detected and separated from their parent cells. Moreover, there are no false separations, that is, all cutlines are located between a bud and a parent cell. The steps of the bud-separation procedure for one cell taken from Figure 4 are illustrated by the images in Figure 6, in which the details are more clearly visible.

To be able to determine the number of cells that do not have a bud, the total number of cells must be determined as well. This number is also used to normalize the numbers of buds in the budding yeast images. The procedure is similar to the bud-counting procedure. The main difference is that the outer boundaries of the cell membranes are utilized instead of the inner boundaries. Because the cells can touch each other, the object separation method must be applied as well. Good results can be obtained with $c < 0.45$ and $r > 3.5$ as the criteria in the object separation method.

3. CASE STUDY

The cell cycle phase distribution of a budding yeast population was estimated using the presented methods. The FACS-based estimation method was used to find the age distribution, and budding index analysis was used to find the time distribution. We used alpha factor-based synchronization, which is a block-and-release-type synchronization method [17]. The *S. cerevisiae* strain Y01408 from Euroscarf (BY4741; MATa; his3D1; leu2D0; met15D0; ura3D0; YIL015w::kanMX4) was used. Samples of the cultivated population were imaged using a light microscope with the sampling interval of 2 minutes, and samples taken with the sampling interval of 6 minutes were analyzed with a FACS. The imaging and FACS analysis were performed for a total of 280 minutes. The details of the experiment as well as all the obtained image and FACS data can be found in the online additional material [15]. Some of the FACS histograms are also presented in Figure 9.

The DNA replication function obtained with (1) is shown in Figure 10. It is interesting to observe that the obtained function is similar to the one that was obtained with noisy simulated data ($\sigma = 0.01$, see Figure 3). Even though we removed clear outliers from the data, that is, we removed the FACS bins beyond the two peaks (as explained above), a significant amount of measurement noise is still present in the remaining data. This can be observed from the shape of the FACS histogram. The peaks, corresponding to the G1 and G2/M phases, are wide, and there is a large number of cells between the peaks. Thus, the proposed estimation method

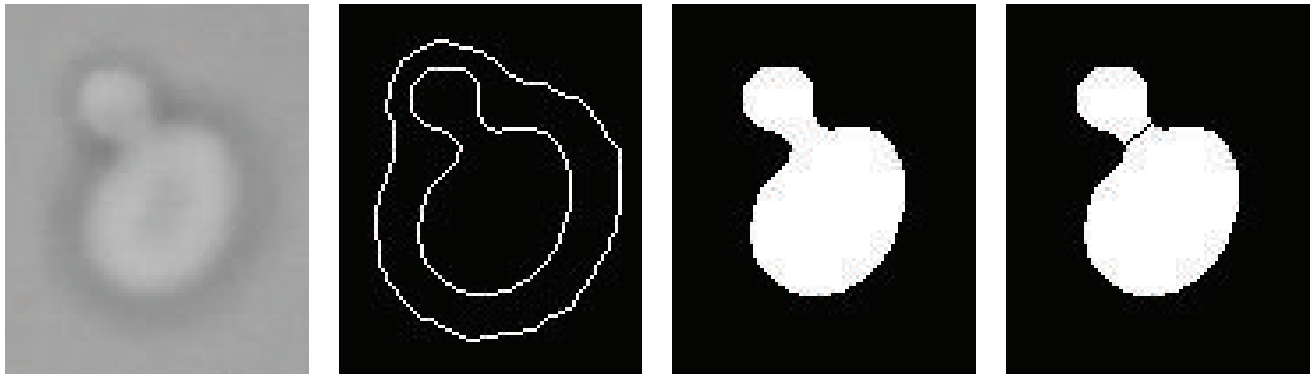

(a) (b) (c) (d)

Figure 6: A part of the image shown in Figure 4 at different image processing stages. The upper left corner is at $(x, y) = (609, 383)$ and the size of the image is 86×105. The image processing stages are (a) original image, (b) segmentation result, (c) result after removing the outer boundary and filling the remaining inner boundary, and (d) bud-separation result.

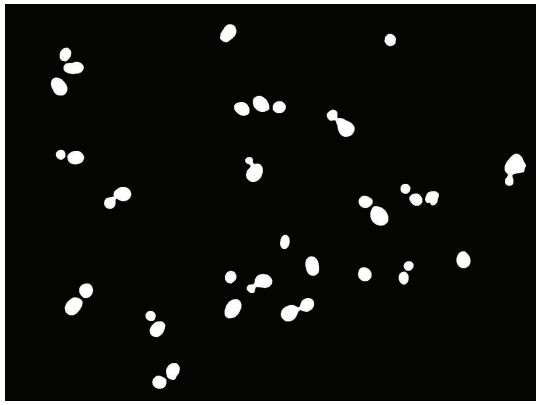

Figure 7: The image shown in Figure 5 after removing objects that touch the edges and filling the objects according to the inner boundary of the cell membrane.

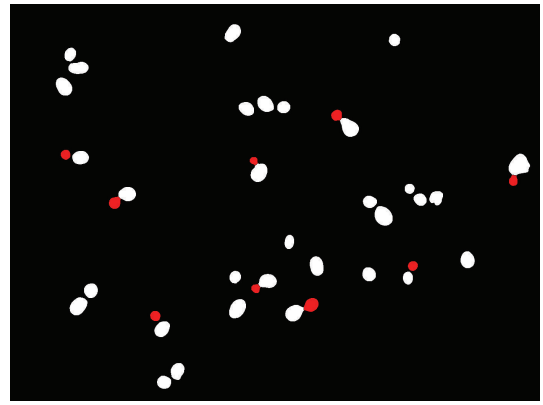

Figure 8: The image shown in Figure 7 after bud separation. The two images are similar, but in this image, buds are not connected to their respective parent cells and are marked with the red color.

works consistently when applied to the real measurement data. The obtained replication function suggests that DNA replication starts at the beginning of the cell cycle and continues in a nearly linear rate throughout the cell cycle. However, this observation is due to the noise in the data. As demonstrated earlier by simulation (see Figure 3), additive noise in FACS measurement biases the estimate towards linear behavior.

The FACS histograms obtained in our experiment suggest that the population was aligned when it was released from alpha factor arrest. The FACS histograms obtained for the first few time instants show a clear peak at the position corresponding to the G1 phase (see the online additional material [15]). This indicates that a majority of the cells have a DNA amount corresponding to N when the population is released from alpha factor arrest. However, once the population is released from alpha factor arrest, the alignment is lost rapidly. This behavior can be observed directly from the FACS histograms, available in the online additional material.

Let us now look at some of the estimated distributions. The age distributions obtained using the FACS-based estimation method are shown in Figure 11. The distributions have been filtered using a mean filter of length 4 to smooth out estimation errors. This filter is able to remove estimation errors caused by numerical problems, but has very little effect on the shape of the filtered distribution. If we look at Figure 11(a), we see that the obtained age distribution shows that a majority of the cells are at an early phase of the cell cycle and a large number of cells are at the middle part of the cell cycle. This is consistent with what is observed directly from the FACS histograms (see Figure 9). Thus, it is clear that the cells start losing alignment rapidly right after the population is released from alpha factor arrest and that cells do not enter the S phase synchronously at the same time. The estimates presented in Figures 11(b) and 11(c) show that over time the majority of the cells have moved to a later phase of the cell cycle, but the alignment is lost even further, which is illustrated by the fact that the corresponding peaks in the distributions have spread.

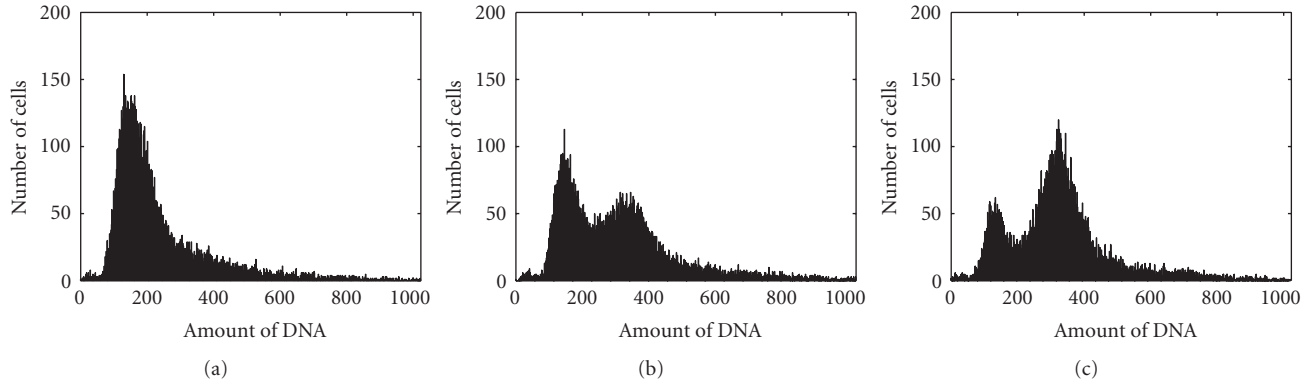

Figure 9: The FACS histograms measured at the time instants: (a) 14 minutes, (b) 44 minutes, and (c) 68 minutes. Corresponding cell cycle phase distribution estimates are shown in Figure 11.

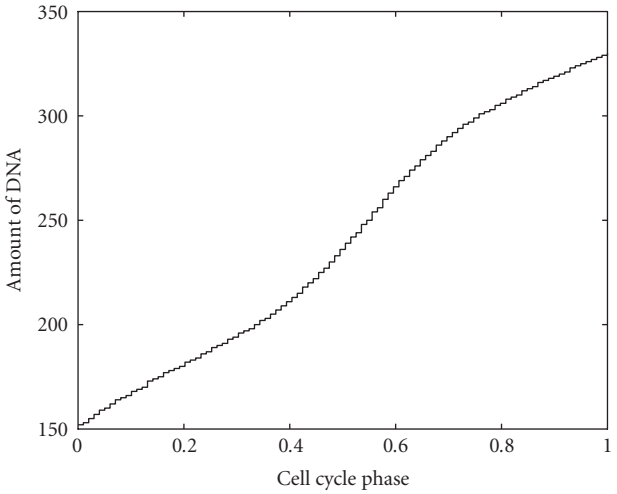

Figure 10: The DNA replication function estimated from an asynchronous FACS histogram from the measurement at the time instant 266 minutes. The amount of DNA corresponds to the quantity shown at the x-axis of the FACS histogram; see, for example, Figure 1.

Automated image analysis was applied to all the images that were obtained in the time series experiment. For each image our method determines the total number of cells and for each cell the size of its bud. The size of the bud is measured in pixels. The cells were divided into three classes: cells that do not have a bud, cells that have a small bud (smaller than one half of the yeast cell), and cells that have a large bud. These classes are assumed to correspond to the cell cycle phases G1, S, and G2/M, respectively. Because our assumption that the size of a bud depends on the phase of the cell cycle is an approximation, the respective time distributions are noisy. The mean filter of length 4 is used to smooth out this noise. The obtained time distributions are shown in Figure 12, in which the number of cells in each class at each time instant is normalized with the number of cells detected at each time instant. The measurement for cells with no bud in Figure 12(a) is very noisy, and no conclusions can be made. The measurements for small and large buds in Figures 12(b) and 12(c) show some alignment: at an early time instant there are a lot of small buds, and at a later time instant there are a lot of large buds.

For comparison, the population estimates obtained using the conventional FACS-based estimation method [7] are shown in Figure 13. Although the data in the FACS and bud-counting datasets are noisy, all three estimation methods show similar alignment in the cell cycle phase distribution of the cells. The data do not show a high degree of synchronization in the way that it should if the population was in perfect synchrony. However, although a good synchronization is not observed, different cell cycle phases can still be observed in the obtained distribution estimates. Thus, due to alpha factor arrest, cells with equal amounts of DNA have aligned to some extent.

4. CONCLUSIONS

Two computational methods for estimating the cell cycle phase distribution of a budding yeast (*S. cerevisiae*) cell population were presented. The methods are based on the analysis of the amounts of DNA in the individual cells of a cell population and on counting the number of buds of a predefined size in microscopic images. The method for analyzing the amounts of DNA is a nonparametric method and does not make any assumptions on DNA replication or the noise characteristics. The image analysis method is fully automated, which ensures objectivity of the image processing results. Neither of the proposed methods makes any assumptions on the synchronization method or the synchrony of the cell population.

The estimated cell cycle phase distributions are discrete distributions. To be able to utilize the distributions for deconvolution of gene expression data, continuous distributions may need to be estimated. For example, an approach for fitting a normal distribution to a discrete distribution has been proposed earlier [7]. Existing deconvolution methods such as the ones published in [6, 7] can benefit from our automated distribution estimation methods.

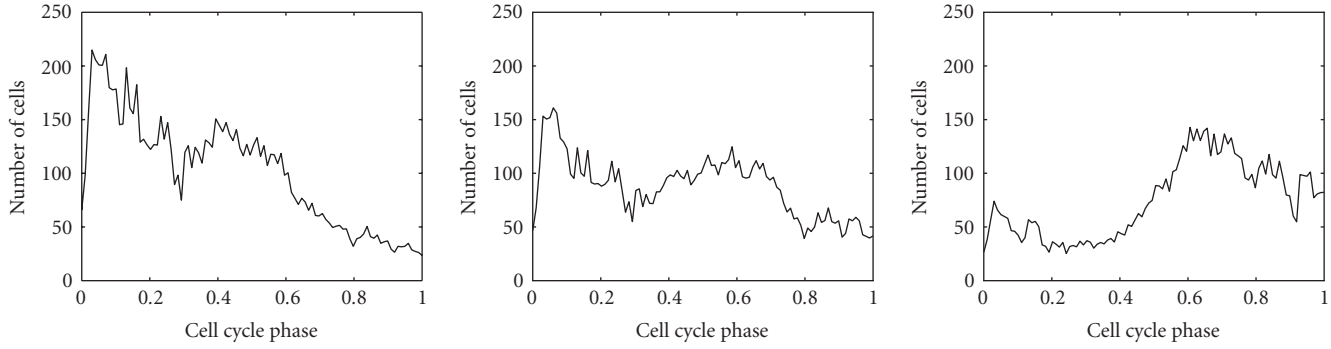

Figure 11: The estimates of the age distributions of the cell population at the time instants (a) 14 minutes, (b) 44 minutes, and (c) 68 minutes as obtained by the proposed approach. The DNA replication function shown in Figure 10 was used to obtain the distribution estimates.

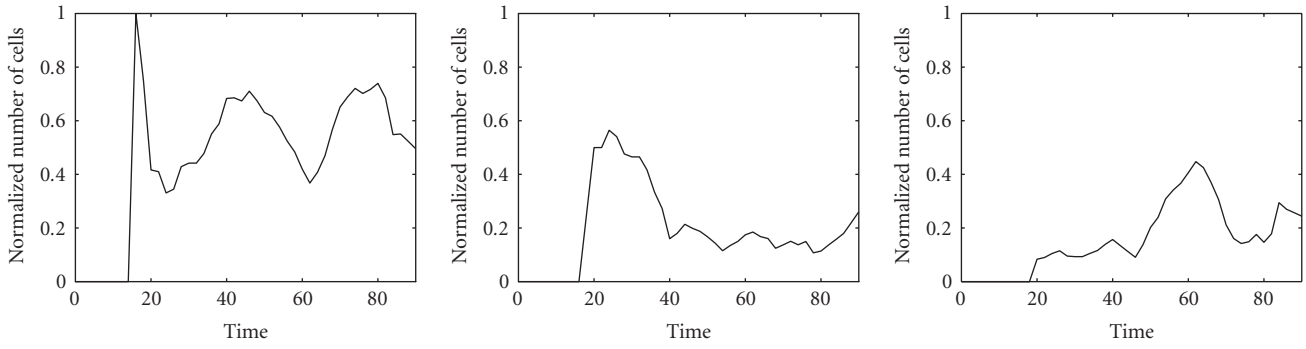

Figure 12: The estimates of the time distributions of the cell population corresponding to (a) cells with no bud, (b) cells with a small bud, and (c) cells with a large bud. The number of cells is normalized with the maximum number of cells. Only the first cell cycle data are shown. Data are not shown for the time instants earlier than 16 minutes because, in the experiment, the microscope was not able to find the correct focus at these time instants. Note that the axes are different from the axes in Figure 11.

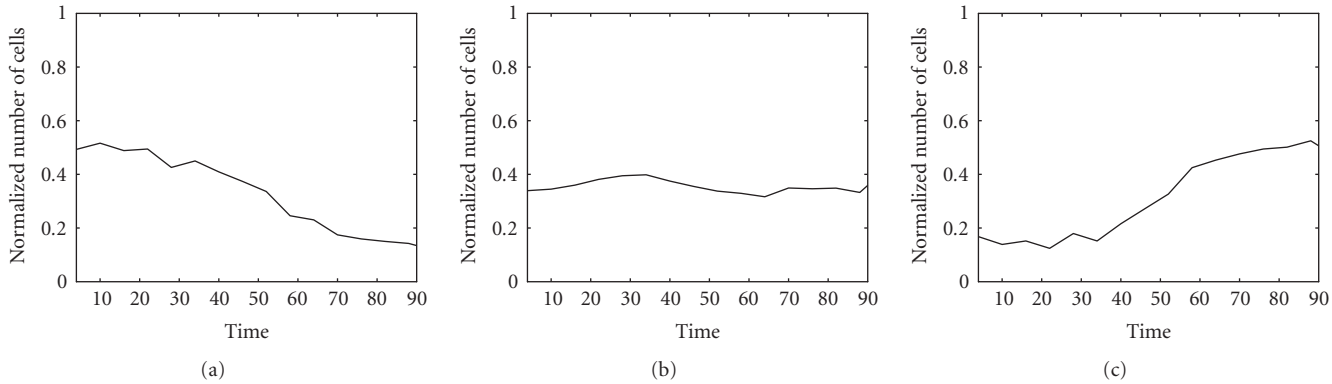

Figure 13: The estimates of the time distributions of the cell population corresponding to the cell cycle phases (a) G1, (b) S, and (c) G2/M as obtained from FACS histograms. The conventional analysis, illustrated in Figure 1, was used to obtain the time distribution estimates. The number of cells is normalized with the maximum number of cells. Only the first cell cycle data are shown. Note that the axes are different from the axes in Figure 11.

ACKNOWLEDGMENTS

The support of the National Technology Agency of Finland (TEKES) and MediCel Ltd. is acknowledged. This work was also supported by the Academy of Finland (application number 213462, Finnish Programme for Centres of Excellence in Research 2006–2011). The first author is supported by the Academy of Finland (application number 120325, Researcher Training and Research Abroad). The authors would also like to thank Juha-Pekka Pitkänen, Ph.D.,

Daniel Nicorici, Ph.D., Jari Niemi, M.S., and Petri Vesanen for their help in the experiment in which the budding yeast data that are used in this paper were produced. The first two authors have contributed equally to this work.

REFERENCES

[1] S. Bornholdt, "Systems biology: less is more in modeling large genetic networks," *Science*, vol. 310, no. 5747, pp. 449–451, 2005.

[2] H. Lähdesmäki, I. Shmulevich, and O. Yli-Harja, "On learning gene regulatory networks under the Boolean network model," *Machine Learning*, vol. 52, no. 1-2, pp. 147–167, 2003.

[3] I. Nachman, A. Regev, and N. Friedman, "Inferring quantitative models of regulatory networks from expression data," *Bioinformatics*, vol. 20, supplement 1, pp. i248–i256, 2004.

[4] J. Tegnér, M. K. S. Yeung, J. Hasty, and J. J. Collins, "Reverse engineering gene networks: integrating genetic perturbations with dynamical modeling," *Proceedings of the National Academy of Sciences of the United States of America*, vol. 100, no. 10, pp. 5944–5949, 2003.

[5] P. T. Spellman, G. Sherlock, M. Q. Zhang, et al., "Comprehensive identification of cell cycle-regulated genes of the yeast *saccharomyces cerevisiae* by microarray hybridization," *Molecular Biology of the Cell*, vol. 9, no. 12, pp. 3273–3297, 1998.

[6] H. Lähdesmäki, H. Huttunen, T. Aho, et al., "Estimation and inversion of the effects of cell population asynchrony in gene expression time-series," *Signal Processing*, vol. 83, no. 4, pp. 835–858, 2003.

[7] Z. Bar-Joseph, S. Farkash, D. K. Gifford, I. Simon, and R. Rosenfeld, "Deconvolving cell cycle expression data with complementary information," *Bioinformatics*, vol. 20, supplement 1, pp. i23–i30, 2004.

[8] M. L. Whitfield, G. Sherlock, A. J. Saldanha, et al., "Identification of genes periodically expressed in the human cell cycle and their expression in tumors," *Molecular Biology of the Cell*, vol. 13, no. 6, pp. 1977–2000, 2002.

[9] A. Lengronne, P. Pasero, A. Bensimon, and E. Schwob, "Monitoring S phase progression globally and locally using BrdU incorporation in TK^+ yeast strains," *Nucleic Acids Research*, vol. 29, no. 7, pp. 1433–1442, 2001.

[10] T. L. Saito, M. Ohtani, H. Sawai, et al., "SCMD: *saccharomyces cerevisiae* morphological database," *Nucleic Acids Research*, vol. 32, Database issue, pp. D319–D322, 2004.

[11] A. Niemistö, T. Aho, H. Thesleff, et al., "Estimation of population effects in synchronized budding yeast experiments," in *Image Processing: Algorithms and Systems II*, vol. 5014 of *Proceedings of SPIE*, pp. 448–459, Santa Clara, Calif, USA, January 2003.

[12] A. Niemistö, M. Nykter, T. Aho, et al., "Distribution estimation of synchronized budding yeast population," in *Proceedings of the Winter International Synposium on Information and Communication Technologies (WISICT '04)*, pp. 243–248, Cancun, Mexico, January 2004.

[13] M. Ohtani, A. Saka, F. Sano, Y. Ohya, and S. Morishita, "Development of image processing program for yeast cell morphology," *Journal of Bioinformatics and Computational Biology*, vol. 1, no. 4, pp. 695–709, 2004.

[14] S. Cooper, "Bacterial growth and division," in *Encyclopedia of Molecular Cell Biology and Molecular Medicine*, R. A. Meyers, Ed., vol. 1, John Wiley & Sons, New York, NY, USA, 2nd edition, 2004.

[15] A. Niemistö, M. Nykter, T. Aho, et al., "Computational methods for estimation of cell cycle phase distributions of yeast cells: online supplement," March 2007, http://www.cs.tut.fi/sgn/csb/yeastdistrib/.

[16] D. Balthasar, T. Erdmann, J. Pellenz, V. Rehrmann, J. Zeppen, and L. Priese, "Real-time detection of arbitrary objects in alternating industrial environments," in *Proccedings of the 12th Scandinavian Conference on Image Analysis*, pp. 321–328, Bergen, Norway, June 2001.

[17] B. Futcher, "Cell cycle synchronization," *Methods in Cell Science*, vol. 21, no. 2-3, pp. 79–86, 1999.